Geo-Resilience 2023 Conference, Cardiff, Wales
D.G. Toll & M.G. Winter (Eds)
British Geotechnical Association, London. 2024
https://doi.org/10.53243/Geo-Resilience-2023-3-6

Load Transfer Mechanism of Single Pile and Monopile-Raft Foundation in Unsaturated Sand

Sonu KUMAR[1], Ashutosh KUMAR[1]

[1]Indian Institute of Technology, Mandi Himachal Pradesh, India
Corresponding author: Ashutosh Kumar (ashutosh@iitmandi.ac.in)

Abstract

The current design practice for single pile (SP) ignores the real case scenario of unsaturated soils present in arid and semi-arid regions of the world. This ignores the contribution of suction in calculating the mobilisation of stresses. However, changing environmental conditions mainly brought by climate change events will change the water regime within the soil thereby dictating the evolution of suction which can cause premature loss of the shear strength of unsaturated soils and alter the serviceability requirement of the foundation systems. The present study implemented the principles of unsaturated soil mechanics using finite element analysis to investigate the load transfer mechanism of SP in unsaturated sand subjected to different hydraulic boundary conditions. A three-dimensional finite element model (3D-FEM) of soil was developed using Plaxis3D. A rigorous fully coupled flow deformation numerical scheme was implemented for solutions. The developed 3D-FEM was validated with the physical modelling result available in the literature, thereafter hydraulic loading in terms of water infiltration (wetting) and evaporation (drying) was applied as a time-dependent net moisture flux boundary condition. The variation of suction stress and its effect on skin resistance and axial stress in SP was analysed. The same analysis was extended to the monopile-raft foundation (MPRF) and the effects of soil-pile-raft interactions on the load transfer mechanism of MPRF were investigated. The results indicated that the location of WT, the evolution of suction stress, and soil water retention behaviour were crucial factors in dictating the mechanical response of SP. In the case of MPRF, the effect of pile-soil-raft interactions governed the load transfer mechanism. The outcome of this study indicates that a climate-resilient foundation design requires incorporating the unsaturated state of the soil.

Keywords: Single pile, Monopile-Raft, Unsaturated Sand, Suction Stress, Hydraulic Loading

1. Introduction

Single pile (SP) foundation is a commonly used deep foundation type and its load transfer mechanism depends upon the mobilization of skin and base resistances (Han et al. 2017). The current design codes and available literature for the design of SP rely on a simplified assumption that the state of soil is either fully dry or completely saturated (BS EN 1997-1: 2004, Eurocode 7; Han et al. 2017). It is to be noted that the monopile-raft foundation (MPRF) is a simplified case of a combined pile-raft foundation system, where the capacities of both SP and raft are utilized and the load transfer mechanism is governed by the soil-pile-raft interactions (Kumar and Choudhury 2018, Kumar and Kumar 2022).

In real scenarios, soils are mostly unsaturated consisting of solid soil particles separated by pores (filled partially by air and water). In conventional practice, the contribution of suction is usually ignored, which leads to conservatism in the design. Suction is the difference between pore air and water pressure ($s = u_a - u_w$) considered as hydrostatically distributed. Suction varies within the soil mass due to evaporation and precipitation brought by soil-atmospheric interaction or due to the fluctuation of the water table (WT). In addition, the climate change events exacerbate the weather events thereby altering the water within the soil which influences the evolution of suction. The resiliency of geo-infrastructure such as pile foundation gets impacted under the extreme weather events thereby threatening the performance of infrastructure. Hence, a design methodology is required to be developed to consider the changing environmental conditions and adopt suitable intervention to safeguard the infrastructure. It is to be noted that soil-atmospheric interaction governs the hydromechanical response of soil due to the exchange of moisture flux. Water evaporation (drying) produces net upward flux and reduces the degree of saturation and vice-versa in case of rainfall infiltration (wetting). Deep percolation of net downward moisture flux would cause the rise in WT. Further, drying/wetting events create transient flow conditions within the unsaturated zone and influences the mechanical behaviour of unsaturated soils such as volume change and shear strength, thereby affecting the pile-soil interaction mechanism. Some experimental studies outlined that suction could improve the ultimate load-bearing capacity of SP by 2-2.5 times (Vanapalli and Taylan 2012). A few studies also suggested using modified shear strength equations at the pile-soil interface for reliable prediction of their load transfer mechanism in unsaturated soils (Hamid and Miller 2009). Wu and Vanapalli 2022 presented the effect of infiltration on the load transfer mechanism of SP in unsaturated soils where settlements and changes in the shaft friction and base resistance were analysed. Few studies were carried out on understanding the behaviour of MPRF in unsaturated soils under hydraulic loading conditions (Kumar and Kumar 2022, 2023).

Finite element analysis (FEA) offers robust mechanisms to solve complex boundary value problems. A prerequisite of the FEA is the adoption of an appropriate constitutive model and estimation of unsaturated soil parameters. Alonso et al. (1990) suggested modified elasto-plastic constitutive models for unsaturated soils incorporating suction as a stress state variable. For these constitutive models, parameters can be obtained using empirical relationships (Vanapalli et al. 1996a, Oh et al. 2009) with the help of soil water retention curve (SWRC) otherwise, unsaturated soil testing is required to obtain the model parameters. Some researchers employed FEA using modified elasto-plastic constitutive models and observed that an improvement in the load bearing mechanism of SP and a MPRF due to the contribution of suction (Kumar and Kumar 2022; Georgiadis et al. 2003). However, studies explaining the load-bearing mechanism of SP and MPRF under infiltration and evaporation events considering the effect of water table change is not explicitly available in literature.

The present study employed a FEA to investigate the load transfer mechanism of SP in unsaturated sand. A three-dimensional finite element model (3D-FEM) of soil and SP was developed using Plaxis3D. The soil was modelled using modified Mohr-Coulomb constitutive relation incorporating Bishop effective stress. The hydro-mechanical model parameters of sand were obtained using empirical relations. The validation of the 3D-FEM was done using the physical modelling result available in literature for saturated and unsaturated conditions. The variation of suction stress and its effect on skin resistance and axial stress of SP was analysed. The study was also extended to the case of monopile-raft foundation and changes in the raft base pressure considering the soil-pile-raft interactions was investigated.

2. Details of the finite element analysis

The elastic perfectly plastic Mohr-Coulomb constitutive model used for saturated/dry soils was modified by incorporating Bishops effective stress σ' (Bishop and Blight, 1963) as per Equations 1 and 2:

$$\sigma' = \sigma + \chi s \quad (1)$$

$$\tau = c + (\sigma + \chi s)\tan\phi' \quad (2)$$

where σ = net total stress; c = apparent cohesion; s = matric suction; ϕ' = angle of shearing resistance. In the present study $\chi = S_{eff}$ was adopted, which enables the transition of the model from unsaturated to saturated state at complete saturation. The term sS_{eff} in the Equation 1 represents the suction stress. The hydromechanical response of soil for drying and wetting was incorporated using the primary drying and wetting soil water retention curves (SWRC). The primary drying curve for Unimin Sand 7030 was adopted from Al-Khazaali and Vanapalli (2019) whereas the wetting SWRC was derived by applying a shift of 25% as per Fredlund et al. (2011).

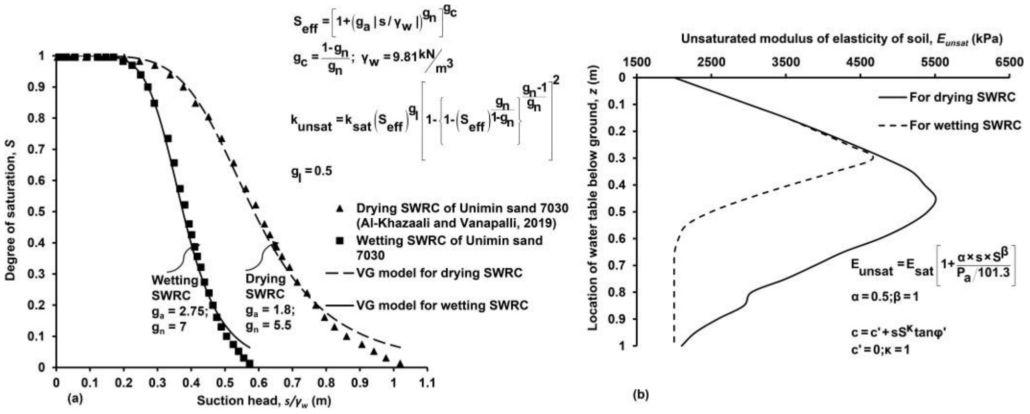

Figure 1: Unimin sand 7030: (a) SWRC fitting using VG model; (b) modulus of elasticity and apparent cohesion.

The van Genuchten (VG) model was used to describe the variation of S_{eff} and unsaturated permeability function k_{unsat} and its empirical parameters (g_a & g_n) were obtained by curve fitting of the SWRCs as shown in Figure 1(a). The location of WT dictated the evolution of initial suction and saturation profile, therefore the strength (c, ϕ') and stiffness (E_{unsat}) parameters of the unsaturated sand were estimated using SWRC employing empirical models given by Vanapalli et al. (1996a) and Oh et al. (2009) as shown in Figure 1(b). Other constitutive model parameters are listed in Table 1.

Table 1: Parameters for Unimin sand 7030 (Data adopted from Al-Khazaali and Vanapalli 2019).

Parameter		Value		
Total unit weight, γ_t (kN/m^3)		18.60		
Saturated unit weight, γ_{sat} (kN/m^3)		20.40		
Angle of shearing resistance, ϕ' (°)		35.3		
Angle of dilation, ψ (°)		3.53		
Poisson's ratio, μ		0.34		
Saturated permeability, k_{sat} (mm/day)		864		
Location of ground water table, z (mm)		0	450	650
Average matric suction, s (kPa)		0	2	4
Apparent cohesion, c (kN/m^2)	Drying SWRC	0	1.35	2.27
	Wetting SWRC	0	0.38	0.47
Elastic modulus, $E_{sat^*/unsat}$ (kN/m^2)	Drying SWRC	2000*	3900	5200
	Wetting SWRC	2000*	3850	2990

3. Development and validation of the finite element model

The SP and MPRF (pile and raft connected as a rigid member) were modelled as linearly elastic isotropic material having modulus of elasticity E_p = 20,000 MPa and Poisson's ratio μ = 0.15. The pile-soil and raft-soil interaction were established using an interface factor R_{int} = 0.67. The mechanical boundary conditions were adopted as fully fixed at bottom and normally fixed at sides and free at top. The hydraulic boundary conditions were opted as closed at bottom and open at sides and ground surface. The mesh discretization was done using 10-noded tetrahedral element. Figure 2(a) provides the model description along with suction variation for WT = 450 mm. Plaxis3D employs Biot's theory of three-dimensional consolidation (Biot, 1941) to describe the flow and deformation behaviour of unsaturated soils. More details on this are available in Kumar and Kumar (2022).

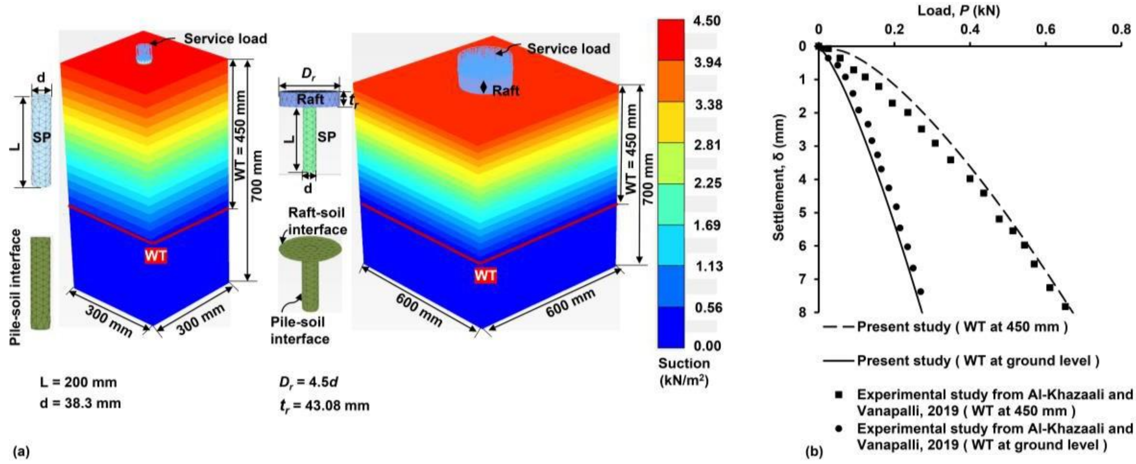

Figure 2: 3D-FEM of (a) SP and MPRF and along with suction profile; (b) load-settlement (P-δ) response of SP.

The validation of the 3D-FEM was performed by obtaining the load-settlement (P-δ) response of SP, where uniform displacement boundary condition was applied in the vertical downward direction at the head of SP for saturated and unsaturated conditions. The unsaturated condition was established by lowering the WT by 450 mm from the ground surface considering impervious moisture flux boundary conditions. The unsaturated soil parameters (c & E_{unsat}) were estimated using primary drying SWRC, where the average suction value (2 kPa) was obtained at the centroid of stressed zone (up to 1.5d below the base of SP). The P-δ response of SP was obtained performing multiple iterations using different mesh sizes. The obtained numerical results showed a good qualitative and quantitative match with the experimental study reported by Al-Khazaali and Vanapalli (2019) as shown in Figure 2(b).

The validated model was extended to MPRF by modifying the lateral dimensions of the soil model by ensuring that the zone of deformation of MPRF is contained within the adopted lateral dimensions. It can be observed that lowering of WT to 450 mm induced a maximum suction of about 4.5 kPa at the ground level and an average suction of 2 kPa at the centroid of stresses zone of SP, which led to an increase in the ultimate load capacity of SP from 0.157 kN to 0.394 kN (i.e., an increase of about 151%). The validated numerical model was used for the further investigation of the effects of hydraulic loading. Prior to the application of hydraulic loading, service load was imposed axially at the head of SP and MPRF in the vertical downward direction. The service load was estimated using a factor of safety (FOS = 3) applied to the ultimate load, whereas ultimate load was obtained from the *P*-δ response of SP corresponds to a vertical displacement of 10% of the pile diameter (δ = 3.83 mm). For MPRF, the diameter of raft (D_r) governs the estimation of ultimate load.

4. Load transfer mechanism for SP

Figure 3 shows the deformation contours of SP subjected to different rates of infiltration. The increment in the rate of infiltration from 10 mm/day to 780 mm/day increased the level of WT from 650 mm to 350 mm from the ground surface which in turn changed the distribution of suction stress. This dictated the mobilisation of skin and base resistances in SP, discussed in the following section.

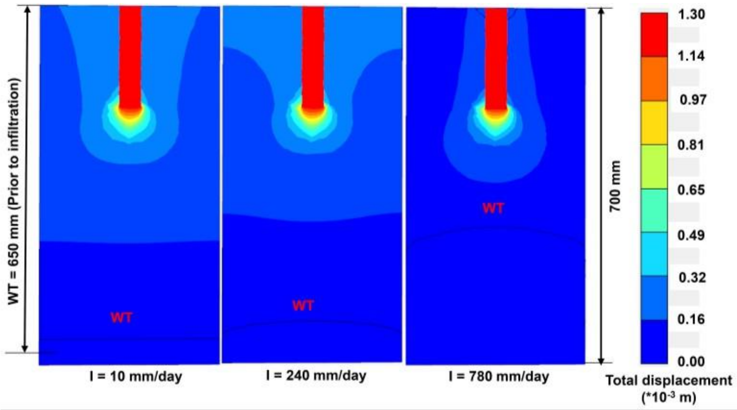

Figure 3: Deformation contours of total displacement for a single pile subjected to infiltration.

4.1 Variation of suction stress

Figure 4 shows the distribution of suction stress sS_{eff} along the soil depth under the 240mm/day of evaporation and infiltration for initial WT locations of 450 mm and 650 mm from the ground surface. It can be observed that the evaporation phenomena reduced sS_{eff} at the ground surface from 3.6 kPa to 2.7 kPa (for initial WT = 450 mm) and from 2.4 kPa to 0.6 kPa (for initial WT = 650 mm) respectively (Figure 4a). The reduction was predominant at the shallow depth. However, an increment in sS_{eff} was observed along the soil depth from 50 mm to 450 mm. This was mainly because of the presence of state of the soil around the initial zone of drying SWRC which dictated the evolution of sS_{eff}.

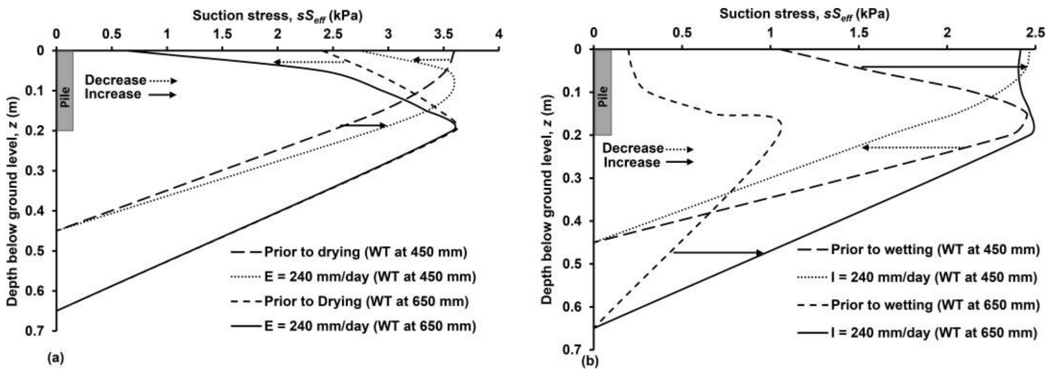

Figure 4: Suction stress for different locations of WT below the ground: (a) evaporation; (b) infiltration.

The infiltration phenomena increased the sS_{eff} at the ground surface (Figure 4b). This is mainly because of increment in the degree of saturation. It has to be pointed out that for WT = 450 mm, sS_{eff} first increased and then reduced along the soil depth when compared to the initial condition. This is due to the presence of the state of the soil on wetting SWRC where higher variation in degree of saturation was observed for WT located at shallow depth compared to deeper depth. Hence, it can be stated that the location of WT table, infiltration and evaporation dictated the evolution of sS_{eff} depending on drying and wetting SWRCs.

4.2 Mobilisation of shaft resistance and axial stress of SP

Figure 5 shows the variation of shaft resistance $f_{s\text{-}SP}$ and the axial stress $f_{p\text{-}SP}$ along the pile length under evaporation and infiltration events for initial WT locations of 450 mm and 650 mm. Results indicate that the mobilisation of $f_{s\text{-}SP}$ was dependent on sS_{eff} (Figure 5a). In case of infiltration, a higher sS_{eff} caused lesser settlement within the soil due to flow-coupled deformation that led to lesser mobilisation of $f_{s\text{-}SP}$. However, in case of evaporation, pile mobilised higher $f_{s\text{-}SP}$ at deeper depth which is mainly because of predominant reduction of sS_{eff} at the shallow depth leading to higher pile-soil relative settlement. These results impacted the $f_{p\text{-}SP}$ distribution along the pile length where a reduction in the $f_{p\text{-}SP}$ distribution led to increment in base resistance for the case of evaporation (Figure 5b). However, increment in the $f_{p\text{-}SP}$ distribution caused reduction in base resistance for the case of infiltration. Such variation was observed for the initial WT location of 450 mm. For initial WT location of 650 mm, the $f_{p\text{-}SP}$ distribution showed a marked increment during the infiltration whereas a negligible variation was observed for the case of evaporation. This is mainly because of marked change in the sS_{eff} along the pile length during the case of infiltration compared to evaporation.

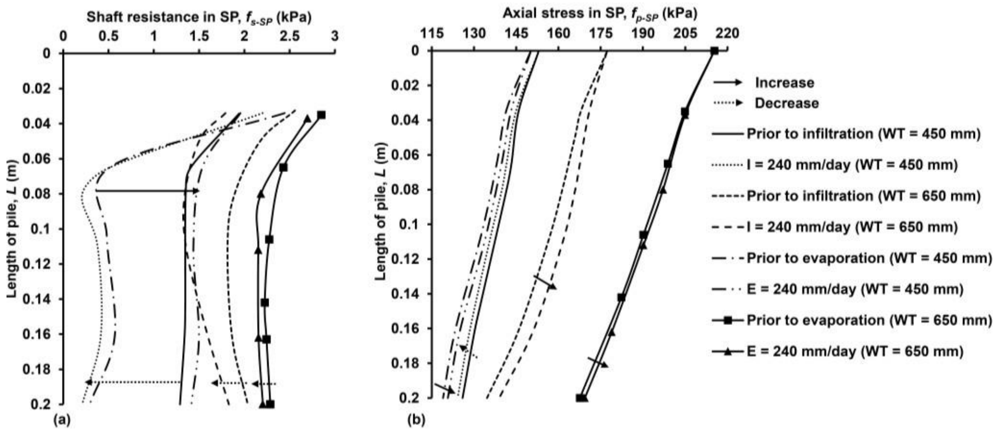

Figure 5: Change in (a) shaft resistance; (b) axial stress along the length of a single pile under hydraulic loading.

5. Mobilisation of axial stress of pile in MPRF

Figure 6 shows the distribution of axial stress in pile of MPRF $f_{p\text{-}MPRF}$ along the pile length under evaporation and infiltration events for the WT locations of 450 mm and 650 mm.

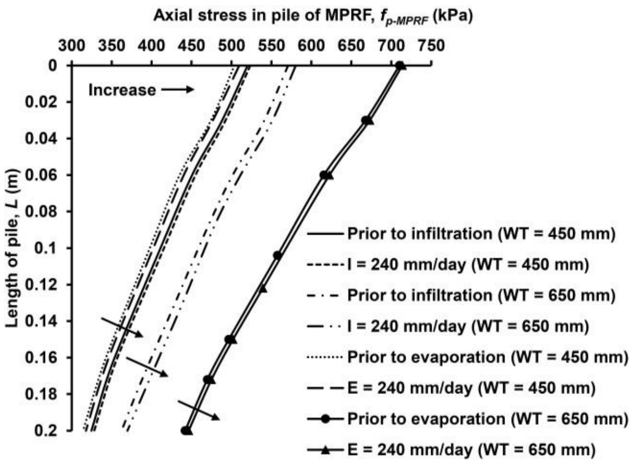

Figure 6: Axial stress along the length in pile of MPRF under hydraulic loading.

The value of $f_{p\text{-}MPRF}$ was higher in case of water table located at deeper depth compared to water table located at shallow depth. This is mainly because of higher level of suction stress in case of water table located at 650 mm below the ground surface. The infiltration and evaporation events reduced the soil-raft interaction which in turn reduced the contact pressure at the raft level thereby increasing the resistance offered by pile.

6. Mobilisation of raft base pressure in MPRF

The mobilization of raft base pressure $Q_{R\text{-}MPRF}$ in MPRF affects the load-sharing between the pile and raft components. Figure 7 shows the distribution of $Q_{R\text{-}MPRF}$ along the raft width from edge of pile to edge of raft under evaporation and infiltration events for both the cases of WT locations. The results indicate non-uniform distribution of $Q_{R\text{-}MPRF}$ under the different rates of infiltration and evaporation. The location of WT predominantly affected the mobilisation of $Q_{R\text{-}MPRF}$ within the raft of MPRF where higher value of $Q_{R\text{-}MPRF}$ was observed for the WT located at 650 mm compared to WT located at 450 mm. This is mainly because of the higher value of sS_{eff} when WT are located at deeper depth. Hence, the presence of WT at deeper depth contributed towards positive raft-soil interaction. In case of evaporation events, the rate of evaporation as well as the location of WT dictated the mobilisation of $Q_{R\text{-}MPRF}$ where a reduction in $Q_{R\text{-}MPRF}$ was observed for WT located at shallow depth whereas an increment in the $Q_{R\text{-}MPRF}$ was observed for WT located at deeper depth. However, the infiltration rates affected mobilisation of $Q_{R\text{-}MPRF}$ where an initial increment and then decrement in $Q_{R\text{-}MPRF}$ was observed which is mainly due to the predominant changes in sS_{eff}.

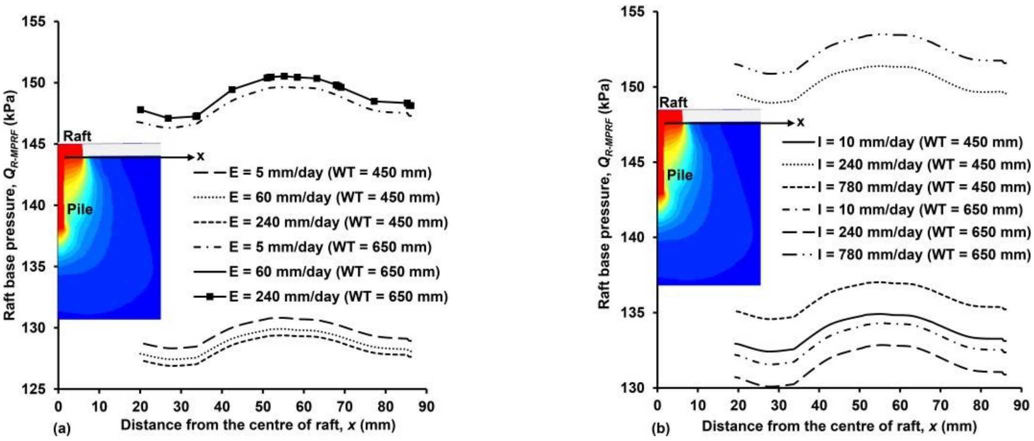

Figure 7: Change in raft base pressure with distance from the centre of raft for (a) evaporation; (b) infiltration.

7. Conclusions

The present study demonstrated the application of the principles of unsaturated soil mechanics in analysing the load transfer mechanism of SP and MPRF in unsaturated sand. This was achieved by developing a three-dimensional finite element model (3D-FEM) of SP, MPRF and soil using Plaxis3D. The elasto-plastic constitutive behaviour of the unsaturated sand was modelled using the elastic perfectly plastic Mohr-Coulomb model modified using Bishops effective stress. The effects of hydraulic loading in terms of rainfall infiltration (wetting) and evaporation (wetting) at different locations of water table was considered. The hydro-mechanical behaviour of unsaturated sand was incorporated using primary drying and wetting SWRC whereas the hydraulic loading was applied as time dependent moisture flux boundary condition. The solutions of the applied boundary conditions were obtained employing fully coupled flow deformation numerical scheme. The obtained results indicated that the location of ground water table, evolution of suction stress and soil water retention behaviour are the crucial factors in dictating the mechanical response of SP and MPRF. The increment in the base resistance of the pile was dependent on the mobilisation of the shaft resistance due to changes in the suction stress brought by infiltration and evaporation events. A reduction in the shaft resistance led to higher mobilisation of base resistance with the piles which is mainly because of higher pile-soil relative settlement. In case of MPRF, contact pressure within the raft was dictated by the location of the ground water table where a higher load with the raft was shared when water table was located at 650 mm below the ground surface. It has to be pointed out that the different rates of infiltration and evaporation changed the pile-soil-raft interaction thereby altering the axial stress mobilisation within the pile of MPRF. The outcome of this study establishes that the soil-atmosphere interaction brought by drying and wetting events can alter the load transfer mechanism within the foundation system and hence such mechanism should be considered while designing the infrastructure in arid and semi-arid regions of the world.

References

Al-Khazaali, M., & Vanapalli, S. K. (2019). Experimental investigation of single model pile and pile group behavior in saturated and unsaturated sand. *J. Geotech. Geoenviron. Eng*., 145(12):04019112.

Alonso, E. E., Gens, A., & Josa, A. (1990). A constitutive model for partially saturated soils. *Géotechnique*, 40(3), 405–430.

Biot, M. A. (1941). General theory of three-dimensional consolidation. *J. Appl. Phys*., 12, 155–164.

Bishop, A. W., & Blight, G. E. (1963). Some aspects of effective stress in saturated and unsaturated soils. *Géotechnique*, 13, 177–197.

BS EN 1997-1: (2004). Eurocode7—Geotechnical design, Part1: General rules, London: British Standards Institution.

Fredlund, D. G., Sheng, D., & Zhao, J. (2011). Estimation of soil suction from soil-water characteristic curve. *Can. Geotech. J*., 48, 186-198.

Georgiadis, K., Potts, D. M., & Zdravković, L. (2003). The influence of partial soil saturation on pile behavior. *Géotechnique*, 53 (1), 11–25.

Hamid, T. B., & Miller, G. A. (2009). Shear strength of unsaturated soil interfaces. *Can. Geotech. J*., 46(5), 595–606.

Han, F., Salgado, R., Prezzi, M., & Lim, J. (2017). Shaft and base resistance of non-displacement piles in sand. *Comput. and Geotech*., 83, 184-197.

Kumar, A., & Choudhury, D. (2018). Development of new prediction model for capacity of combined pile-raft foundations. *Comput. and Geotech*., 97, 62-68.

Kumar, S., & Kumar, A. (2022). Effect of infiltration on single pile and mono pile-raft foundation embedded in unsaturated sand. *Int. J. Geomech*., 04022288-12. https://doi.org/10.1061/IJGNAI.GMENG-7908.

Kumar, S., & Kumar, A. (2023). Behaviour of Single Pile and Mono Pile-Raft Foundation under Hydraulic loading Considering Hysteresis in Unsaturated Sand. *Geo-Congress 2023*, Los Angeles, California, USA, (Accepted).

Oh, W. T., Vanapalli, S. K., & Puppala, A. J. (2009). Semi-empirical model for the prediction of modulus of elasticity for unsaturated soils. *Can. Geotech. J*., 46 (8), 903–914.

Plaxis 3D V20.04 [Computer software]. Delft, Netherlands.

Van Genuchten, M. T. (1980). A closed-form equation for predicting the hydraulic conductivity of unsaturated soils. *Soil Sci. Soc. Am. J.,* 44:892-898.

Vanapalli, S. K., Fredlund, D. G., Pufahl, D.E., & Clifton, A. W. (1996b). Model for the prediction of shear strength with respect to soil suction. *Can. Geotech. J*., 33(3),379–392.

Vanapalli, S. K., & Taylan, Z. N. (2012). Design of single piles using the mechanics of unsaturated soils. *Int. J. Geomate*., 2(1), 197-204.

Wu, X., & Vanapalli, S. K. (2022). Three-dimensional modelling of the mechanical behavior of a single pile in unsaturated expansive soils during infiltration. *Comput. and Geotech*., 145, 104696.